SENRA Academic Publishers, Burnaby, British Columbia
Vol. 3, No. 1, pp. 751-754, 2009
ISSN: 1715-9997

Canadian Journal of pure & applied sciences

DETECTION OF SOLAR AND TERRESTRIAL PHENOMENA BY 40 KHZ SUBIONOSPHERIC VLF SIGNAL: REPORT

*S S De[1], B Bandyopadhyay[1], B K De[2], D K Haldar[1] and Suman Paul[1]
[1]Centre of advanced Study in Radio Physics and Electronics
1, Girish Vidyaratna Lane, Kolkata 700 009
[2]Department of Physics, Tripura University, Tripura 799 130, India

ABSTRACT

At Agartala (Lat 23° N, Long 91° 24´ E), North-Eastern part of India, continuous monitoring of VLF/LF sferics and subionospheric transmitted signals are being continued since 1975. From the recording of one such subionospheric signal at 40 kHz from Japan (Lat 36° 11´ N, Long 139° 51´ E), some observed typical variations in the transmitted signal amplitude during solar flares and meteor showers will be presented in this paper.

Keywords: VLF signal modulation, solar flare effects, meteor shower detection.

INTRODUCTION

Solar X-ray flares, meteor showers, geomagnetic storms and other terrestrial phenomena while entering the earth's atmosphere produce electromagnetic waves in the VLF range due to interaction with the medium, which propagate and reach the ground at the same instance as the optical signals (Price and Blum, 2000; De *et al*., 2006; Chakrabarti *et al*., 2002; Keay, 1995; Beech *et al.*, 1995).

The effects of large electric field from any such origin introduce perturbation in ion composition, temperature and other physical parameters within the ionosphere at different levels of altitude extending from the lowest D-region to the magnetosphere height. Anomalous changes of amplitude and phase of VLF subionospheric signals would occur during their propagation through such perturbed regions (Volland, 1982; Rodger, 2003; Dowden and Adams, 1990; Garaj *et al*., 2000; Nickolaenko *et al*., 1999). From VLF amplitude and phase observations, solar flare induced ionospheric D-region changes have been investigated (Nickolaenko and Hayakawa, 1998; Thomson and Clilverd, 2000).

Wave propagation below 300 kHz within the earth-ionosphere wave-guide is characterized by complex phenomena involving nonhomogeneous and anisotropic media. In recent period, based on FDTD computational solutions of Maxwell's equations, the effects of anomalous electric field during solar and different geophysical events upon subionospheric wave propagation are being successfully analysed (Thomson and Cliverd, 2001; Baba and Hayakawa, 1995; Otsuyama *et al*., 2003; Simpson and Taflove, 2004).

In this paper, some typical variations of amplitude of 40 kHz subionospheric Japanese signal due to solar flares and meteor showers will be presented. These are recorded at Agartala (Lat 23° N, Long 91° 24´ E) at different periods over the past twenty years.

*Corresponding author email: de_syam_sundar@yahoo.co.in

The Features of the 40 kHz Sub-ionospheric Signal

Transmitter call sign JG2AS/JJF-2

Location	**Japan**
Latitude	36° 11´ N
Longitude	139° 51´ E

Transmitting antenna

Type	Omni-directional
Power at radiation	10 kW
Operation	Continuous

Receiver

The recording system consists of loop antenna feeding a number of OP-AMPs used in tuned radio frequency mode. The output of the AC amplifier is detected and the DC level is further amplified logarithmically. The DC gain has been used to adjust the receiver's sensitivity corresponding to the incoming signal which shows marked variation over the year. The DC output is used as the signature of the amplitude of 40 kHz signal. The overall gain of the amplifier is 120 dB with a band width of 200 Hz. The time constant of the recorder is 7.5 sec. A gyrator-II type VLF receiver has also been made useful for recording this signal (Simpson and Taflove, 2007). Using computer sound card, data were recorded at a sample rate of 10/s which have been analyzed through origin 5.0.

Observed Sub-ionospheric signals from Agartala

The diurnal behavior of the amplitude of 40 kHz signals under normal condition is depicted in figure 1. In the figure, the zones A, B, C and D represent sunrise minima, recovery effect, afternoon maxima and sunset minima, respectively.

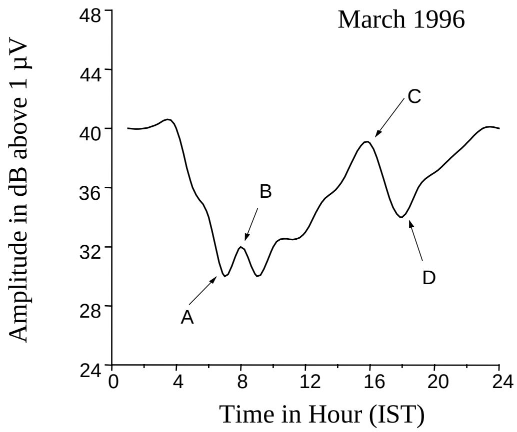

Fig. 1. Diurnal behavior of amplitude of 40 kHz radio signal.

Figure 2 shows a typical enhancement in signal strength due to solar flare in 40 kHz in relation to Sudden Enhancement in Signal Strength, SES, occurred during 0854 Hour to 0916 Hour on 24.01.2007. Here, C: commencement time and E is the end of the event.

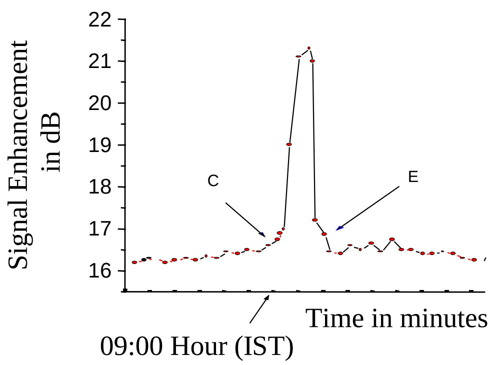

Fig. 2. Typical enhancement in signal strength due to solar flare.

During solar flare, the signal level rises and follows the sequences of enhanced solar radiation. This has been termed as SES.

Some of the observed SES

Occurrences of SES in different solar phases P1, P2, P3 and P4 and their relationship with different types of X-ray flares:

P1: The Sun moves from Tropic of Cancer to Equator (21 June-21 September)

P2: The Sun moves from Equator to Tropic of Capricorn (22 September-21 December)

P3: The Sun moves from Tropic of Capricorn to Equator (22 December-21 March)

P4: The Sun moves from Equator to Tropic of Cancer (22 March-21 June).

Solar cycle	Solar Phase	Percentage association of SES with X-ray flares of types		
		Impulsive	GRF	Spikes
22nd	P1	81	85	65
	P2	78	81	62
	P3	72	78	58
	P4	68	75	56
23rd	P1	79	79	61
	P2	74	76	57
	P3	68	72	54
	P4	65	68	51

Some correlation studies are presented in figure 3.

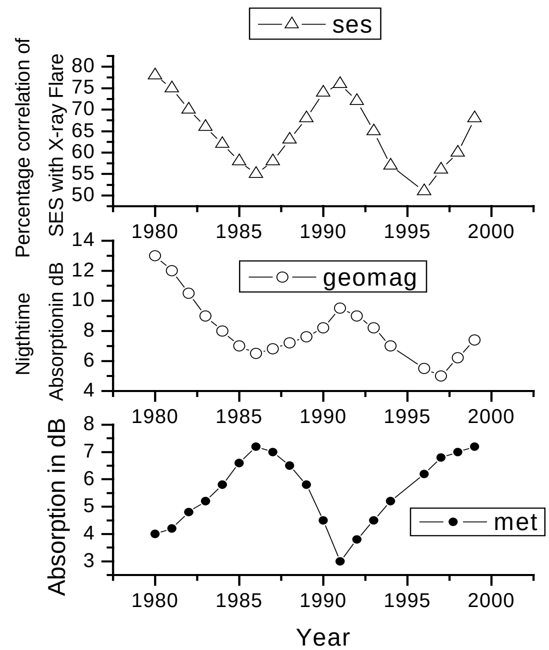

Fig. 3. Three graphs show the percentage correlation of SES, average nighttime absorption in geomagnetically active days and average absorption in sporadic meteorologically active days in various years of 21st- 22nd, 22nd-23rd solar cycles.

The results show good correlation with solar cycle variations. But the magnitudes are solar cycle dependent. It is seen that the effects are slightly higher in 21st – 22nd solar cycle than in 22nd – 23rd solar cycle.

Solar Cycles

Solar cycles are shown in figure 4.

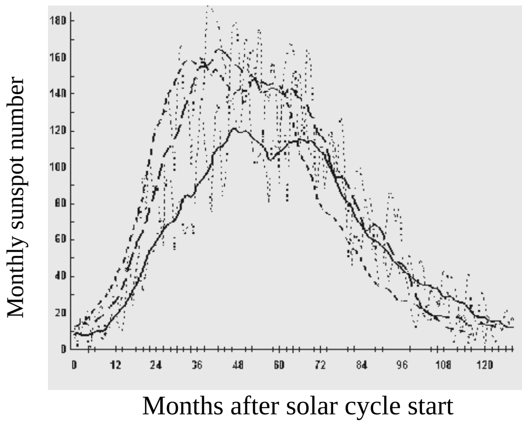

Fig. 4. Different solar cycles.

Monthly smoothed sunspot number
21: Large dashed line curve
22: Small dashed line curve
23: Solid line curve

Actual monthly sunspot number
21: 22: 23: Shown by the corresponding dotted curve

- Cycle 21 started in June 1976 and lasted 10 years and 3 months.
- Cycle 22 started in September 1986 and lasted 9 years and 8 months.
- Cycle 23 started in May 1996.

The sunspot numbers during solar cycles are the representative points of the absorption of 40 kHz signal.

Leonid Meteor Showers
The Leonid meteor showers of 1998 have been presented in figure 5 by recording its effects on 40 kHz Japanese subionspheric signal over Agartala. The shower exhibited peak activities on Nov. 16, 1998. Detection of meteor showers by recording their effects on transmitted signals had been reported earlier from Kolkata (Lat 22° 34´ N, Long 88° 30´ E) at some other frequencies (De *et al.*, 2006; Chakrabarti *et al.*, 2002).

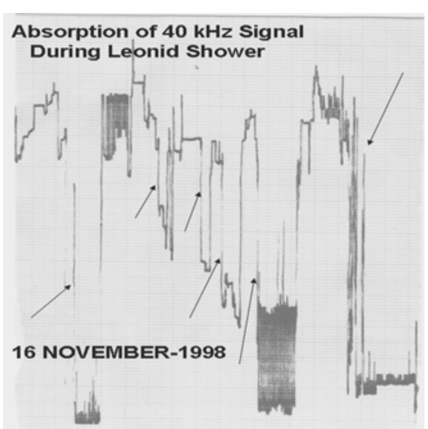

Fig. 5. Typical Leonid meteor shower of 16 November, 1998.

At 40 kHz signal frequency, the influences of atmospherics were relatively much lower compared to lower frequencies. The signal strength is sufficiently strong for detection over Agartala having great circle distance at 4884 km.

The day from 15 to 21 November, 1998 had very clear sky and no serious 'thunder-bolt' related events were reported at Agartala. So apart from the solar terrestrial influences on the ionosphere, the period was ideal for observing meteor showers. Moreover, no solar flare events were reported around the period of occurrence by GOES10 and GOES12 satellites which continuously monitor solar activity. At the predicted peak activity period, there were no local lightning or flare generated perturbations in the ionosphere that could alter the average signal received at Agartala.

The extra ionization produced by the supersonic meteoroids during their passage through lower ionosphere was the cause of high enhancement of signal level, which is about eight to nine times the normal value.

During the entry of the Leonid into the earth's atmosphere, there will be strong fluctuation of charge distribution in the medium which enhances the rate at which the energy gets randomized. As a result, instability is produced. For this, the relative electron-ion drift velocity may exceed the value for the onset of Kelvin-Helmholtz instability. The compressible ionospheric plasma driven by velocity shears and earth's magnetic field at the frontal path of the meteor increases the growth rate of Kelvin-Helmholtz instability thereby generating electromagnetic waves that produce the observed effects in the subionospheric signal.

ACKNOWLEDGEMENT

This work is funded by Indian Space Research Organization (ISRO) through S K Mitra Centre for Research in Space Environment, University of Calcutta, Kolkata, India.

REFERENCES

Price, C. and Blum, M. 2000. ELF/VLF Radiation Produced by the 1999 Leonid Meteors. Earth, Moon and Planets. 82-83:545-554.

De, SS., De, BK., Guha, A. and Mandal, PK. 2006. Detection of 2004 Leonid meteor shower by observing its effects on VLF transmission. Indian J. Radio and Space Phys. 35**:**396-400.

Chakrabarti, SK., Pal, S., Acharya, K., Mandal, S., Chakrabarti, S., Khan, R. and Bose, B. 2002. VLF observation during Leonid meteor shower-2002 from Kolkata. Indian J. Phys. 76B (6):693-697.

Keay, CSL. 1995. Continued Progress in Electrophonic Fireball Investigations. Earth, Moon and Planets. 68:361-368.

Beech, M., Brown, P. and Jones, J. 1995. VLF detection of fireballs. Earth, Moon and Planets. 68:181-188.

Volland, H. 1982. Handbook of Atmospherics. Eds. Volland, H. CRC Press, Boca Raton, Fla. 179-250.

Rodger, CJ. 2003. Subionospheric VLF perturbations associated with lightning discharges. J. Atmos. Sol. Terr. Phys. 65:591-606.

Dowden, RL. and Adams, CDD. 1990. Lightning - induced perturbations on VLF subionospheric transmissions. J. Atmos. Sol. Terr. Phys. 52:357-363.

Garaj, S., Vinkovic, D., Zgrablic, G., Kovacic, D., Gradecak, S., Biliskov, N., Grbac, N. and Andreic, Z. 2000. Observational detection of meteor-produced VLF electromagnetic radiations. FIZIKA A (Zagreb). 8:91-98.

Nickolaenko, AP., Hayakawa, M., Kudintseva, IG., Myand, SV. and Rabinowicz, LM. 1999. ELF subionospheric pulse in time domain. Geophys. Res. Lett. 26:999-1002.

Nickolaenko, AP., Hayakawa, M. 1998. Natural electromagnetic pulses in the ELF range. Geophys. Res. Lett. 25:3101-3106.

Thomson, NR. and Clilverd, MA. 2000. Solar cycle changes in daytime VLF subionospheric attenuation. J. Atmos. Sol. Terr. Phys. 62:601-608.

Thomson, NR. and Clilverd, MA. 2001. Solar flare induced ionospheric D-region enhancements from VLF amplitude observations. J. Atmos. Sol. Terr. Phys. 63: 1729-1737.

Baba, K. and Hayakawa, M. 1995. The effect of localized ionospheric perturbations on subionospheric VLF propagation on the basis of finite element method. Radio Sci. 30:1511-1518.

Otsuyama, T., Sakuma, D. and Hayakawa, M. 2003. FDTD analysis of ELF wave propagation and Schumann resonances for a subionospheric waveguide model. Radio Sci. 38: doi: 10.1029/2002RS002752.

Simpson, JJ. and Taflove, A. 2004. Three-dimensional FDTD modeling of impulsive ELF propagation about the Earth-sphere. IEEE Trans: Antennas and Propag. 52: 443-451.

Simpson, JJ. and Taflove, A. 2007. A Review of Progress in FDTD Maxwell’s Equations Modeling of Impulsive Subionospheric Propagation Below 300 kHz. IEEE. Trans. Antennas and Propag. 55:1582-1590.